

# Wood Cutting with a Pendulum Dynamometer (VI) —Relation among Cutting Energy, Cutting Force and Type of Chip Formation—

H. SUGIHARA,<sup>\*,\*\*</sup> M. NOGUCHI<sup>\*\*</sup>, S. OKUSHIMA,<sup>\*\*</sup> and K. NOMURA<sup>\*\*</sup>

杉原彦一<sup>\*,\*\*</sup>, 野口昌己<sup>\*\*</sup>, 奥島俊介<sup>\*\*</sup>, 野村憲治<sup>\*\*</sup>: 振り子式木材切削試験器による  
木材切削に関する研究 (第6報)  
切削所要エネルギー, 切削力ならびに切削型の関係

## 1. Introduction

In some studies,<sup>1)2)3)4)5)</sup> effects of wood species, cutting direction, depth of cut, moisture condition, tool angle, clearance angle and rake angle on energy consumption in wood cutting by means of a pendulum dynamometer, have been already reported.

The present study was made to investigate the relation between the energy consumption measured with the pendulum dynamometer and the cutting force (main and radial component) measured with the electrical resistance strain gage. And also the relation between the type of chip formation and the variation of cutting force was observed by using a high speed-camera, and strain gage and oscillograph. Furthermore, two pendulums of different weight were used in order to investigate if the weight of the pendulum influenced the measured energy consumption or not.

## 2. Apparatus of Experiment

The pendulum dynamometer was used to measure the energy consumption. The principle and the procedure of this experimental method were closely described in a previously published paper.<sup>1)</sup>

The electrical strain gage was used to measure the cutting force (main and radial component). And the cutting force was recorded as the wave by the oscillograph. Two gages method was adopted in order to aim at the thermal compensation and to double the sensitivity of the strain gage. So a total of four gages among which two gages are to measure the main component and the other two gages to measure the radial component were mounted on the load cell as shown in Fig. 1. The knife was fixed at the pendulum as a cantilever. Fig. 1 shows the load cell, the knife- and gage-mounting method. And further the pendulum dynamometer was

\* Division of Wood Physics (木材物理研究部門)

\*\* Department of Wood Science and Technology, Kyoto University (京都大学農学部)

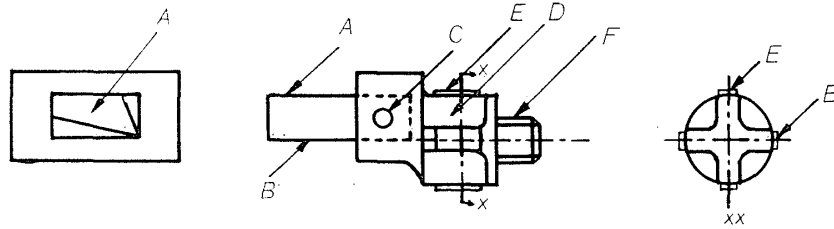


Fig. 1. load-cell, knife and gage

A : knife                      B : cutting edge      C : screw for knife  
 D : strain detector      E : strain gage      F : screw for load cell

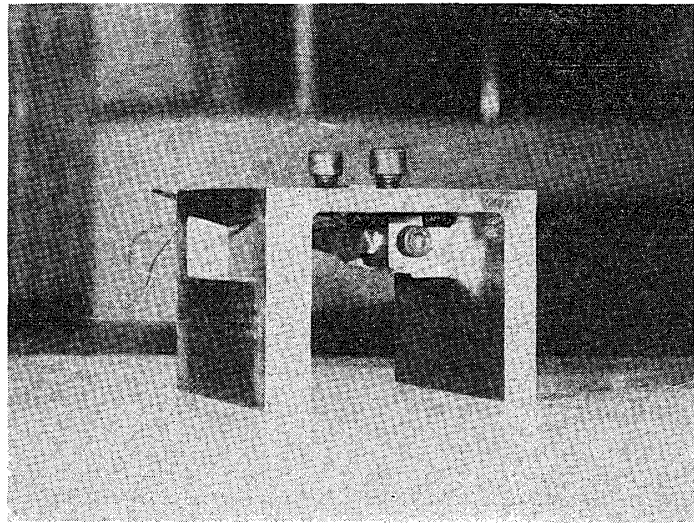
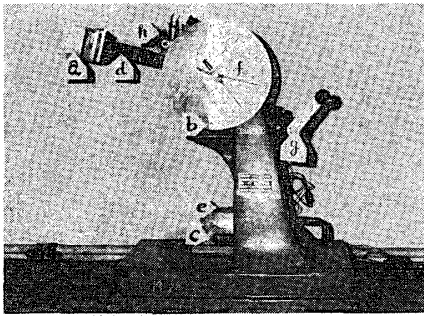


Photo. 1. pendulum dynamometer

reconstructed as shown in Photo. 1 in order to set up this load cell on the pendulum.

The relation between the type of chip formation and the variation of cutting force was investigated by using high speed-camera (Shimadzu high speed-camera KS-16) together with oscillograph (Yokogawa MA-33). The weight of the used pendulum are 1.862 kg and 3.135 kg.

### 3. Experimental Factor

#### A. cutting direction

Three kinds of cutting direction were adopted, that is, cross sectional cutting (C) (bark to pith), radial sectional cutting parallel to the fiber (hereafter referred to by  $R_{f//}$ ) and radial sectional cutting perpendicular to the fiber (hereafter referred to by  $R_{f\perp}$ ). Fig. 2 shows these cutting directions.

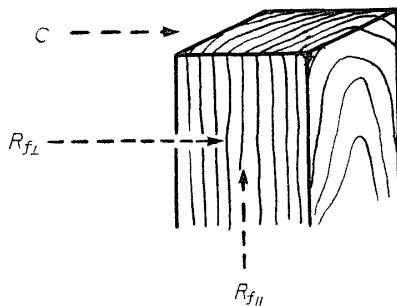


Fig. 2. cutting direction

#### B. depth of cut (d)

Three levels of depth of cut (0.10 mm, 0.25 mm, 0.40 mm) were adopted.

**C. moisture condition (c)**

Air dried specimen and water saturated one were adopted. The moisture contents of specimens are shown in Table. 1.

Table 1. Condition of Wood Specimen

speies	moisture content of air dried specimen (%)	moisture content of water saturated specimen (%)	specific gravity of oven dried specimen	density of annual ring, number of annual ring/mm
Japanese cypress	17.9	216.0	0.44	21/20
beech	17.4	124.0	0.65	20/20
Japanese oak	18.7	89.8	0.83	13/20
red lauan	18.3	245.1	0.41	
kapor	19.5	106.9	0.75	

**D. cutting length (S)**

The cutting lengthes were 10 mm, 20 mm and 30 mm. The forms of the cutting surface are shown in Fig. 3.

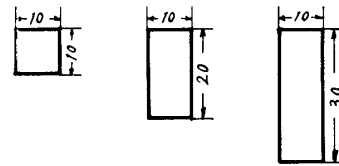


Fig. 3. forms and dimension of cutting surface

**E. weight of the pendulum (capacity of dynamometer)**

The pendulums of 1.862 kg (5 lb ft) and 3.135 kg (10 lb ft) were used.

**F. wood species**

Choosing the wood species for this experiment, the following matters were considered; comparing the result of this experiment with the previous one and taking the wood species which are used frequently in wood industry. Thus Japanese cypress (*Chamaecyparis obtusa* Sieb. et Zucc), Japanese oak (*Quercus crispula* Blume), beech (*Fagus crenata* Blume), lauan (*Shorea negrosensis* Foxw) and kapor (*Dryyobalanops*, sp.) were adopted.

**G. rake angle**

The tool angles were 65°, 55°, 45° and 35°, and the rake angle were 10°, 20°, 30° and 40°, so the clearance angle was constant, 15°. But the rake angle of the 1.862 kg pendulum were 13°, 23°, 33° and 43°, and the clearance angle was constant, 12°, because the part in which the knife was inserted was not so accurately worked.

**4. Result and Discussion**

The results of this experiment are shown in Fig. 4~19 and analyzed by the method of the analysis of variance.

**4. 1 Relation between Energy Consumption and Cutting Force**

When the main component is referred to by  $P(s)$  and the cutting length by  $S$ ,

the energy consumption  $E_0$  is given by

$$E_0 = \int_0^S P(s) ds \quad (1)$$

And when the mean main component is referred to by  $P_0$ , equation (1) will be transformed to

$$E_0 = \int_0^S P(s) ds = P_0 S \quad (2)$$

$$P_0 = \frac{1}{S} \int_0^S P(s) ds$$

The relation between  $E_0$  and  $P_0$  is shown in Fig 4, 5, 6. Here,  $E$  is the energy consumption which was measured by the pendulum dynamometer and corresponds to ordinate in the graph. The mean main component corresponds to abscissa. The relation between  $E$  and  $P_0$  is linear, but the straight line does not pass through the origin and it crosses the  $E$  axis at a positive value. So the following equation can be introduced by the equation (2).

$$E = E_0 + \Delta E \quad (3)$$

$$= P_0 S + \Delta E \quad (3')$$

The relation between  $E$  and  $S$ , however, is given by

$$E = k \cdot S^5 \quad (4)$$

Here,  $k$  is constant.

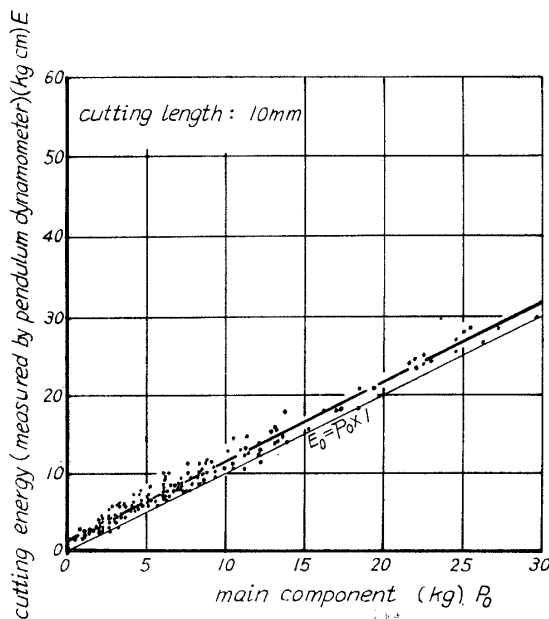


Fig. 4. relation between cutting energy  $E$  and main component  $P_0$

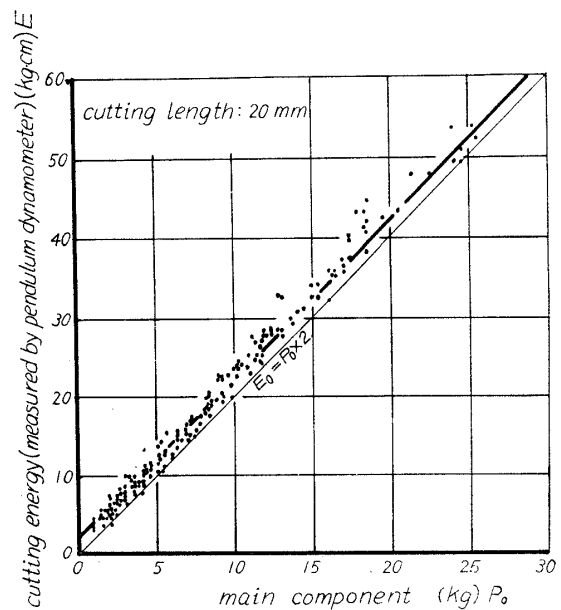


Fig. 5. relation between cutting energy  $E$  and main component  $P_0$

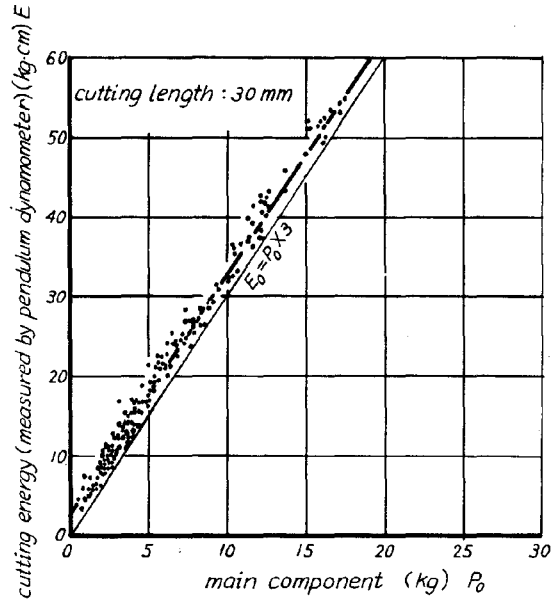


Fig. 6. relation between cutting energy  $E$  and main component  $P_0$

As  $\Delta E$  must be a linear function of  $S$  according to the equation (3') and (4), (3') is transformed to

$$E = P_0 S + \Delta E = P_0 \cdot S + \lambda S = (P_0 + \lambda) \cdot S \quad (5)$$

$$\Delta E = \lambda \cdot S$$

Here,  $\lambda$  is constant.

On the other hand as shown in Fig. 7, it seems that the relation between  $\Delta E$  and  $S$  is linear and that the straight line passes through the origin.

The causes of  $\Delta E$  will be thought as follows.

1) When the edge strikes against the specimens, loss energy  $\Delta E_1$  is occurred by the impact. :  $\Delta E_1$

2) The locus of the cutting edge is bow shaped as shown in Fig. 8. As the result of this fact, the real cutting length is 30.10mm as for the specimen of 30mm. So the real energy consumption is not  $P_0 \times 30$ , but  $P_0 \times 30.10$  (Kg mm).

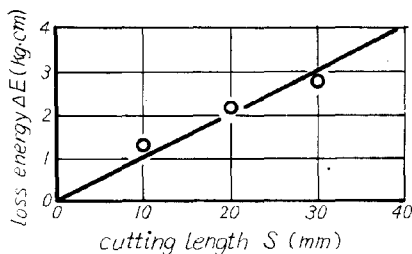


Fig. 7. relation between loss energy  $\Delta E$  and cutting length  $S$

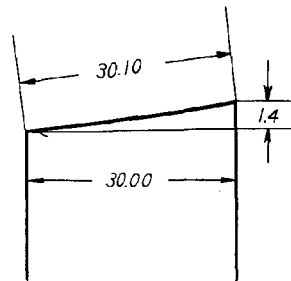


Fig. 8. locus of cutting edge

And  $\Delta E_2 = P_0 \times (30.10 - 30.00)$  kg mm. :  $\Delta E_2$

The real cutting length of 20 mm specimen is 20.08 mm and that of 10 mm specimen is 10.01 mm.

3) The frictional resistance on the rotating axis is increased by the radial component. :  $\Delta E_3$

These phenomena are piled up and  $\Delta E$  may be as

$$\Delta E = \Delta E_1 + \Delta E_2 + \Delta E_3 + \dots$$

#### 4. 2 Radial Component (Vertical Component) V

The tendency that the radial component (V) in the cross-sectional cutting is negative (the direction to which the knife presses down the specimen) is remarkable, but that tendency in  $R_{r//}$  and  $R_{r\perp}$  cutting is not remarkable as shown in Fig. 9. Furthermore when this phenomenon is observed in detail, in cross-sectional cutting, V in the case of small depth of cut (0.10 mm) is positive, but V decreases rapidly with the increasing depth of cut and becomes negative. Also in  $R_{r//}$  and  $R_{r\perp}$  cutting V decreases, but it does not become negative in the range of this experiment (0.10 mm-0.40 mm). As for beech and Japanese oak V becomes negative at small depth

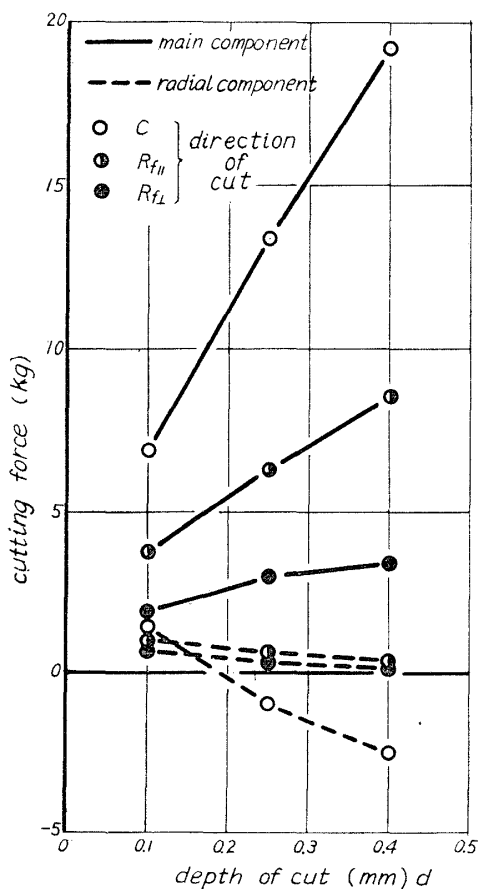


Fig. 9. relation between cutting force and depth of cut

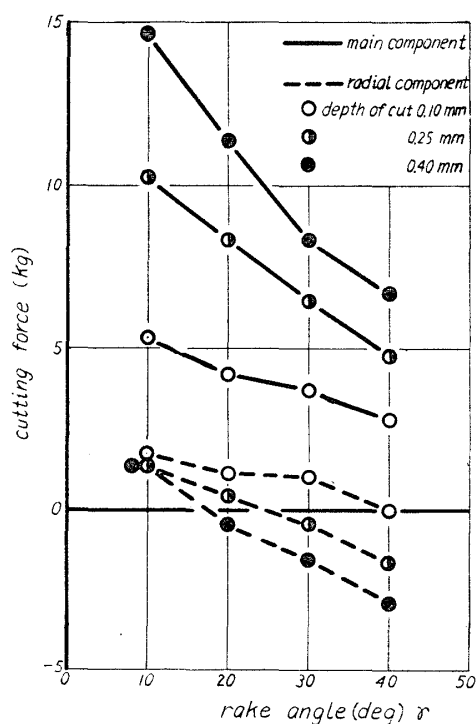


Fig. 10. relation between cutting force and rake angle

of cut (about 0.15 mm) in cross-sectional cutting.  $V$  decreases and changes from positive to negative with the increasing rake angle (with the decreasing tool angle) as shown in Fig. 10.

But when the depth of cut is small (0.10 mm),  $V$  does not become negative in the range of this experiment ( $10^\circ \sim 40^\circ$ ).

In cross-sectional cutting  $V$  decreases rapidly with the increasing rake angle and becomes negative. In  $R_{f//}$  and  $R_{f\perp}$  cutting  $V$  decreases with the increasing rake angle, but the tendency is not so remarkable.

$V$  of the air dried specimen is larger than that of the water saturated specimen, but the difference between them becomes little with the increasing rake angle as shown in Fig. 11.

And then the rake angle at which  $V$  is zero, that is, the critical rake angle, is referred to by  $\gamma_0$ .  $\gamma_0$  of beech and Japanese oak are larger than that of the other wood species. Fig. 12 shows that  $\gamma_0$  decreases with the increasing depth of cut and that in cross-sectional cutting  $\gamma_0$  decreases rapidly between 0.10 mm and 0.25 mm. And also  $V$  in cross-sectional cutting becomes zero at the smaller depth of cut than that in the other cutting directions as shown in Fig. 9.

The follow is the consideration of the above mentioned observation. Cutting resistances which are consisted of the distribution-load on the face and the flank of the knife are assumed to be divided into normal force to the face and the flank of the knife ( $N, N'$ ) and parallel one to the face and the flank ( $T, T'$ ).  $R$  is the result-

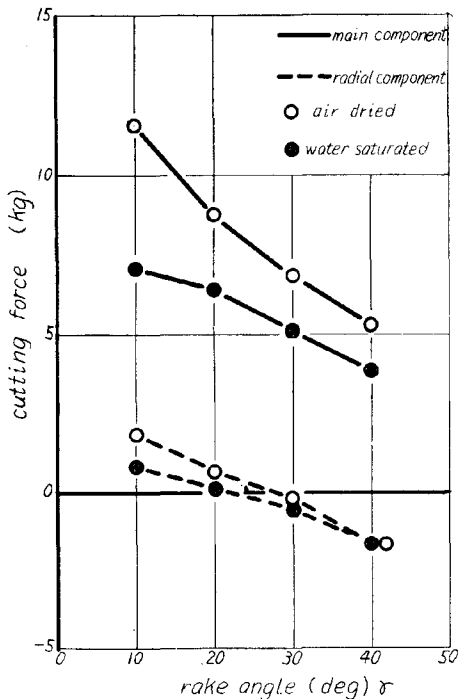


Fig. 11. relation between cutting force and rake angle

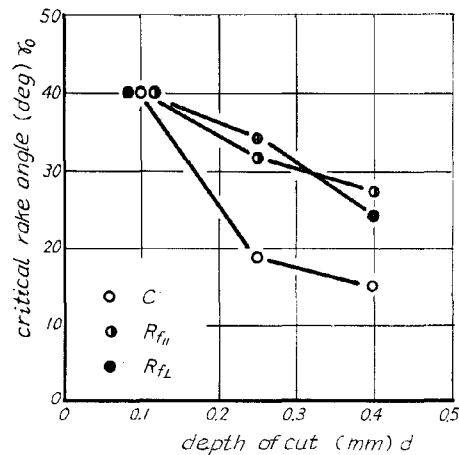


Fig. 12. relation between critical angle ( $\gamma_0$ ) and depth of cut ( $d$ )

ant force of them. (see Fig. 13)

And then  $\rho$ ,  $\rho'$  are defined as follows.

$$\tan\rho = T/N \quad \tan\rho' = T'/N'$$

The relation between the main component  $P$  and the radial component  $V$  are given by using  $\rho$  and  $\rho'$

$$V = P \tan(\rho - \gamma) \tag{6}$$

$$V = P \tan(\rho' - \alpha) \tag{7}$$

Here,  $\gamma$  is the rake angle and  $\alpha$  is the clearance angle.

When the relation between  $P$  and  $V$  is discussed as for the rake angle  $\gamma$ , equation (6) must be used and as for the clearance angle  $\alpha$  equation (7) must be used. In this paper  $V$  is discussed by using equation (6).

According to equation (6), whether  $V$  is negative or positive is decided by the relation between  $\rho$  and  $\gamma$ . If  $\rho$  is constant, it is decided only by  $\gamma$ . However, as it is clear from the result of this experiment, whether  $V$  is negative or positive is decided not only by  $\gamma$ , but also by the depth of cut ( $d$ ), the moisture condition ( $c$ ), the cutting direction and the wood species. Fig. 14 shows that  $\rho$  is influenced by these factors.

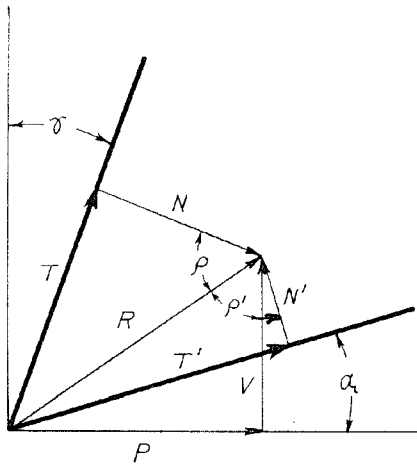


Fig. 13. cutting resistance

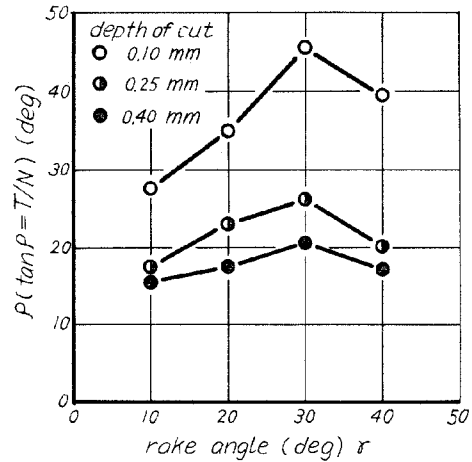


Fig. 14. relation between  $\rho$  and rake angle  $\gamma$

It is reasonable that the so called friction angle is influenced by the moisture content, the cutting direction and the wood species.  $\rho$ , however, is influenced also by the depth of cut as shown in this experiment. This fact is considered as follows. It seems that the property of the produced surface of the chip and the specimen changes with the depth of cut.

In cross-sectional cutting  $\rho$  is comparatively small and  $\rho$  is often smaller than  $\gamma$ . And  $\rho$  decreases with the increasing depth of cut (Franz, Saito and Kobayashi



reported the same).<sup>6)7)</sup> So it seems that the tendency of  $V$  to be negative becomes remarkable with the increasing depth of cut. In cross-sectional cutting it is due to the large value of  $P$  that  $V$  does not change to negative when the depth of cut is small.

The result in this experiment is almost the same as Nakamura and Aoyama's report.<sup>8)</sup> They, however, report that  $V$  is zero under the condition of 0.50 mm depth of cut and  $40^\circ$ – $50^\circ$  tool angle, but in this report the tool angle at which  $V$  is zero is about  $65^\circ$  when the depth of cut is 0.50 mm. This difference, about  $20^\circ$ , between this report and their report may arise from the kind of the wood species which were used in these experiments, because the critical rake angle  $\gamma_0$  changes with the wood species. Under the condition of 0.10 mm depth of cut and  $15^\circ$  clearance angle, the critical angle,  $40^\circ$  is not influenced by the cutting direction.

#### 4. 4 Type of Chip Formation and Cutting Force

In the case of the cross-sectional cutting of the air dried specimen the tear type is occurred regardless of the depth of cut. The main component of the tear type is the largest and its variation is rather larger and irregular as shown in Photo 2 and Fig. 15. On the other hand the radial component is small and changes irregularly. But it seems that the type of chip formation of the water saturated specimen changes from the tear type to the broken type with the increasing rake angle and depth of cut. In the case of  $R_{f//}$  cutting of the small depth of cut, the flow type is occurred regardless of the rake angle, but it changes to the broken type, or it has the advanced

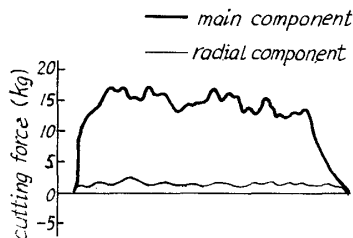


Fig. 15. cutting force of tear type  
 $C$ , 0.2mm (depth of cut)  
 $10^\circ$  (rake angle), dry, Japanese cypress

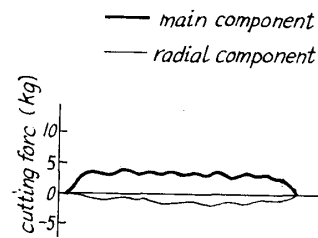


Fig. 16. cutting force of flow type  
 $R_{f//}$ , 0.2mm,  $10^\circ$ , dry,  
 Japanese cypress

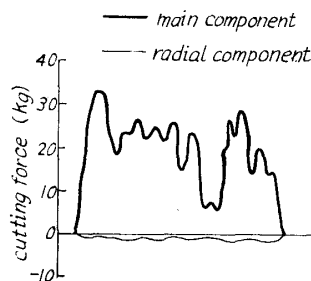


Fig. 17. cutting force of broken type  
 $R_{f//}$ , 0.5mm,  $10^\circ$ , dry,  
 Japanese cypress

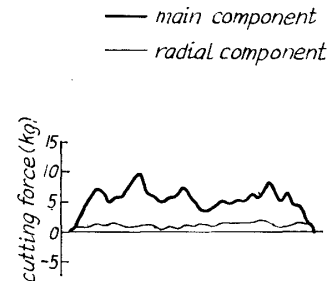


Fig. 18. cutting force of shear type  
 $R_{f\perp}$ , 0.5mm,  $10^\circ$ , dry,  
 Japanese cypress

splitting with the increasing depth of cut and rake angle. The main component of the flow type is the smallest and its variation is little and regular as shown in Photo 3 and Fig. 16. On the other hand it seems that the radial component is rather small and constant. The broken type has the main component of the largest variation which becomes almost zero when the edge reaches the base of the advanced splitting, but the variation of the radial component is small in comparison with that of the main component. (see Photo 4 and Fig. 17)

In the case of  $R_{f\perp}$  cutting of the small depth of cut and the low rake angle the shear type is occurred. But the type of chip formation changes from the shear type to the broken type or the flow type with the increasing rake angle. With the increasing depth of cut, however, it changes to the broken type. The shear type has the main component of the similar, large and irregular variation as that of the tear type, and the radial component has rather large variation as compared with that of the other types as shown in Photo 5 and Fig. 18.

The effect which the rake angle gives to the main component is changed by the cutting direction. In the case of  $R_{f//}$  cutting the main component is very much influenced by the rake angle as compared with the other two cutting direction. As this reason the follows will be considered. In this cutting direction the face of the knife is always pressed by the flow type-chip or the broken type-chip. On the other hand the chips of the cross-sectional cutting or  $R_{f\perp}$  cutting are wood meal or splin-

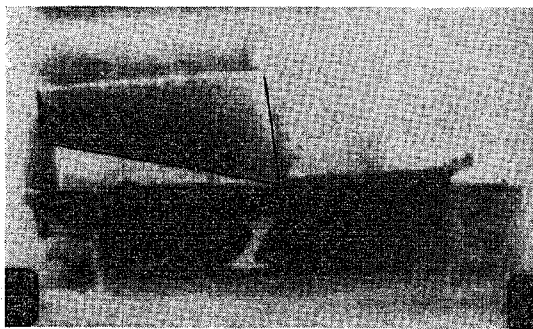


Photo. 2. tear type cutting direction C

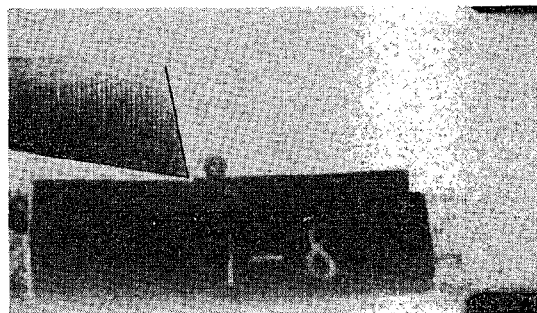


Photo. 3. flow type  $R_{f//}$

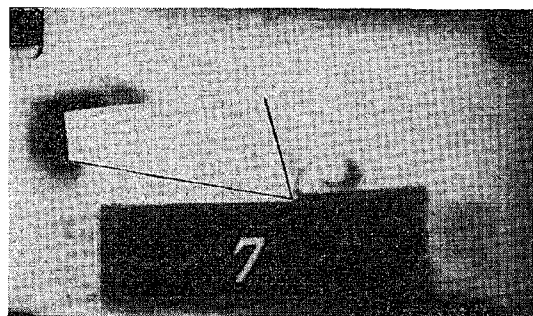


Photo. 4. broken type  $R_{f//}$

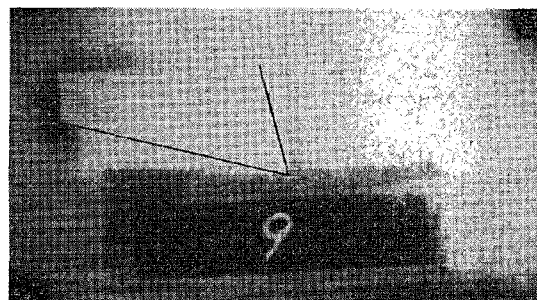


Photo. 5. shear type  $R_{f\perp}$

ters, so it seems that they scatter. This fact is shown by the high speed-camera. (see Photo 2, 3, 4 and 5)

Furthermore there is no relation between the negative or positive of the radial component and the type of chip formation.

#### 4. 5 Effect of Weight of Pendulum

In this experiment, to investigate whether the weight of the pendulum influences on the measured energy consumption or not, the pendulum of 1.862 Kg (5 lbft) and 3.135 Kg (10 lbft) were used. The result is shown in Fig. 19.

#### 5. Conclusion

1) The relation between the energy consumption  $E$  measured by the pendulum dynamometer and the mean main component of cutting force  $P_0$  can be given by

$$E = E_0 + \Delta E$$

$$E_0 = P_0 \cdot S, \quad \Delta E = \lambda \cdot S$$

Here,  $S$  is cutting length and  $\lambda$  is constant.

2) In the case of the cross-sectional cutting the tendency of the radial component to become negative is remarkable, but in the case of the  $R_{f//}$  and  $R_{f\perp}$  cutting this tendency is not remarkable. The radial component decreases and is apt to become negative with the increasing depth of cut and rake angle. The radial component in air dried specimen is larger than in water saturated one.

3) The critical rake angle decreases with the increasing depth of cut. The critical rake angle is constant,  $40^\circ$ , under the condition of the 0.10 mm depth of cut and the  $15^\circ$  clearance angle, regardless of the cutting direction and the wood species. So it seems that this cutting condition is convenient for the comparison of the machinability of the wood.

4) In the case of the cross-sectional cutting the type of chip formation is the tear type and in the case of the  $R_{f//}$  cutting it is the flow type when the depth of cut is small, but it changes to the broken type with the increasing depth of cut. In the case of the  $R_{f\perp}$  cutting it is the shear type when the depth of cut is small, but it changes to the broken type with the increasing depth of cut.

5) The weight of the pendulum does not influence decisively on the measured energy consumption.

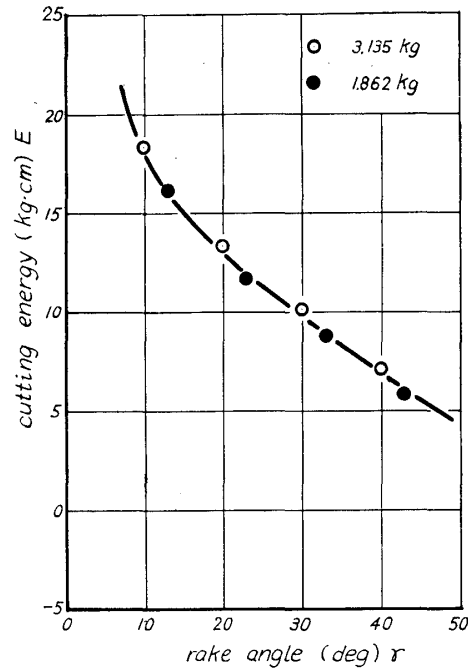


Fig. 19. relation between cutting energy and rake angle

### Acknowledgement

The authors want to express their gratitude to Mr. YOSHIDA for making many test specimens and also to Mr. KOBAYASHI and Mr. OH-I who have carried out the preliminary experiment of this study as the graduation thesis of the Department of Forestry, Kyoto Uni., in 1965.

### 摘 要

振子式木材切削試験器により木材の切削所要エネルギーを測定し、同時に試験器の刃物固定部にストレインゲージをはりつけて切削力（主分力、背分力）を測定し、切削所要エネルギーと平均主分力の関係、ならびに背分力について調べた。さらに高速度カメラを用いて切削型を観察し、切削型と切削力の関係についても検討してみた。その結果次のことが明らかになった。

- 1) 試験器で測定された切削所要エネルギー  $E$  と平均主分力  $P_0$  の関係は次の式で示される。

$$E = E_0 + \Delta E$$

$$E_0 = P_0 \cdot S, \quad \Delta E = \lambda \cdot S$$

ただし  $S$  は切削長さ

$\lambda$  は定数

2) 木口面切削において背分力は負になる傾向が強いが、 $R_{f//}$ ,  $R_{f\perp}$  方向切削ではその傾向は強くない。切り込み深さが大きくなると、あるいはすくい角が大きくなると背分力は減少して負になりやすい。また臨界すくい角は切り込み深さが増加すると小さくなる。

3) 木口面切削における切削型はむしろ型、 $R_{f//}$  方向切削では流れ型、切り込み深さが大きくなると折れ型になる。 $R_{f\perp}$  方向切削では一般に剪断型である。

- 4) 振子重量は切削所要エネルギーに影響をあたえない。

### Literature Cited

- 1) SUGIHARA, H. and M. NOGUCHI, Wood Research, No. 28, 31 (1962).
- 2) NOGUCHI, M. and H. SUGIHARA, and etc., JOURNAL OF THE JAPAN WOOD RESEARCH SOCIETY, 8, 260 (1962).
- 3) NOGUCHI, M., H. SUGIHARA, and etc., Wood Research, No. 30, 1 (1963).
- 4) NOGUCHI, M., H. SUGIHARA, and etc., JOURNAL OF THE JAPAN WOOD RESEARCH SOCIETY, 10, 10 (1964).
- 5) NOGUCHI, M., H. SUGIHARA, and etc., Wood Research, No. 34, 45 (1965).
- 6) FRANZ, N.C., Analysis of the wood cutting process, The University of Michigan Press, (1958).
- 7) KOBAYASHI, A. and K. SAITO, Journal of polymer Science, 58, 1377 (1962).
- 8) NAKAMURA, G. and T. AOYAMA, BULLETIN OF THE GOVERNMENT FOREST EXPERIMENT STATION, No. 93, 69 (1957).